Supporting Information

Surface enrichment of iridium on IrCo alloy for boosting hydrogen production

Ngoc Kim Dang[a], Muhammad Umer[a], Pandiarajan Thangavel[a], Siraj Sultan[ab], Jitendra N. Tiwari[a], Jong Hoon Lee[c], Min Gyu Kim[d] & Kwang S. Kim*[a]

[a]*Center for Superfunctional Materials, Department of Chemistry, Ulsan National Institute of Science and Technology (UNIST), 50 UNIST-gil, Ulsan, 44919, Korea.*

[b]*School of Energy & Chemical Engineering, UNIST, Ulsan, 44919, Korea*

[c]*UNIST Central Research Facilities, Ulsan, 44919, Korea*

[d]*Beamline Research Division Pohang Accelerator Laboratory (PAL) Pohang 37673, Korea*

*Email address: kimks@unist.ac.kr

Materials

Iridium chloride hydrate ($IrCl_3.xH_2O$), Cobalt acetate tetrahydrate ($Co(acac)_2.4H_2O$), Cobalt(II) chloride hexahydrate ($CoCl_2.6H_2O$), D-Glucose (G8270), Melamine (M2659), Nafion were suppled from Sigma-Aldrich. 95% Sulfuric acid (H_2SO_4), Nitric acid (HNO_3) and ethanol were purchased from SAMCHUN Chemical. Carbon Black – Vulcan XC-72R was supplied by FuelCellStore. 20 % Pt on Vulcan XC-72 and 20 % Ir on Vulcan XC-72 were purchased from Premetek. Toray Carbon paper PTFE treated TGP-H60 was supplied by Alfa Aesar.

Calibration of reference electrode

The electrolyte (0.5 M H_2SO_4) was saturated by bubbling hydrogen gas for at least 30 min before calibration.[1] The measured potentials versus saturated calomel electrode (SCE) were converted to the potentials versus reversible hydrogen electrode (RHE) by the following equation:

$$E_{RHE} = E_{SCE} + 0.2603 \text{ V}$$

Turnover frequency calculation

The TOF per metal (Ir-based) site in the **IC1-G$_N$** catalyst for the HER is estimated by the equation:

$$TOF = \frac{Total\ number\ of\ hydrogen\ turnover/geometric\ area\ (cm^2)}{Number\ of\ active\ sites/geometric\ area\ (cm^2)}$$

The total number of hydrogen turnovers was calculated from the current density using the formula.

$$Number\ of\ hydrogens = j(mA\ cm^{-2})1(Cs^{-1}(10^{-3}mA)^{-1})(1\ mol\ e^{-}(96485.3\ C)^{-1})(\frac{1\ mole\ H_2}{2\ mole\ e^{-}})(\frac{6.022\ x\ 10^{23}\ molecules\ H_2}{1\ mole\ H_2})$$

$$= 3.12\ x\ 10^{15}\ H_2\ s^{-1}cm^{-2}\ per\ mA\ cm^{-2}$$

The number of Ir metal ions was determined from the inductively coupled plasma-optical emission spectroscopy (ICP-OES) measurement (5 wt%).

Accordingly, the active site density based on bulk Ir is:

$$\frac{5}{100}\ x\ (1.6\ mg\ cm^{-2})\ x\ \left(\frac{1\ mmol}{192.2\ mg}\right) x\ 6.022\ x\ 10^{20}\ sites\ mmol^{-1}$$

$$= 2.5\ x\ 10^{17}\ Ir_{sites}cm^{-2}$$

At an overpotential of 0.0293 V (vs RHE), the HER current density is 100 mA cm^{-2}, and the Ir based TOF value of catalyst was calculated to be

$$\frac{3.12\ x\ 10^{15}\ H_2\ s\ cm^{-2}\ mA^{-1}\ cm^2\ x\ 100\ mA\ cm^{-2}}{2.5\ x\ 10^{17} Ir_{sites} cm^{-2}} = 1.248\ s^{-1}/Ir_{sites}$$

Mass activity calculation

Mass activity of the catalysts were calculated by following formula:

$$\text{Mass activity } \frac{A}{mg} = \frac{current\ density\ (\frac{A}{cm^2})}{sample\ loading\ on\ electrode\ surface\ \left(\frac{mg}{cm^2}\right) * Ir\ (or\ Pt)con}$$

Take **IC1-G$_N$** for an example, mass activity of **IC1-G$_N$** was estimated at 29.3 mV vs RHE

$$\text{Mass activity } \frac{A}{mg_{Ir}} = \frac{0.1\ A}{\frac{5 * 60}{1000 * 0.25} * 5.0132\%} = 1.662\ A\ mg_{Ir}^{-1}$$

Geometry Model and Computational Method

Model

The primitive unit cells of individual metal surfaces were optimized using 11x11x1 *k*-point and then we built a 5-layered 3×3-supercells of each unit cell (Pt-111, Ir-111, Co-111 and 1:1 ratio of Ir-Co-111). The bottom two layers of metal atoms were fixed at the bulk lattice positions, whereas the top three layers and the adsorbed hydrogen were relaxed. A vacuum space of 15 Å was set in the z-axis to eliminate the interactions between the neighboring layers.

Computational Method

All calculations were carried out by using Vienna Ab-initio Simulation Package (VASP).[2] Spin-polarized density functional theory (DFT) calculations were performed using revised PBE (RPBE)[3] with the Tkatchenko–Scheffler dispersion correction (TS)[4] and projected augmented-wave pseudopotentials[5] with the kinetic energy cutoff of 500 eV. The Brillouin zone was sampled by a 3×3×1 array of *k*-points in the Γ-centered grid. All structures were fully relaxed to the ground state. The convergences of energy and force were set to 1×10^{-4} eV and 0.02 eV/Å, respectively. H-adsorption energies (ΔE_{H^*}) was calculated by $\Delta E_{H^*} = E_{H-Surface} - (E_{Surface} + 0.5E_{H_2})$ and the free energies (ΔG_{H^*}) were obtained by using $\Delta G_{H^*} = \Delta G_{H^*} = \Delta E_{H^*} + \Delta ZPE - T\Delta S$, where ΔE_{H^*} is the hydrogen adsorption energy, ΔZPE and ΔS are the zero point energy changes and entropy changes, respectively.

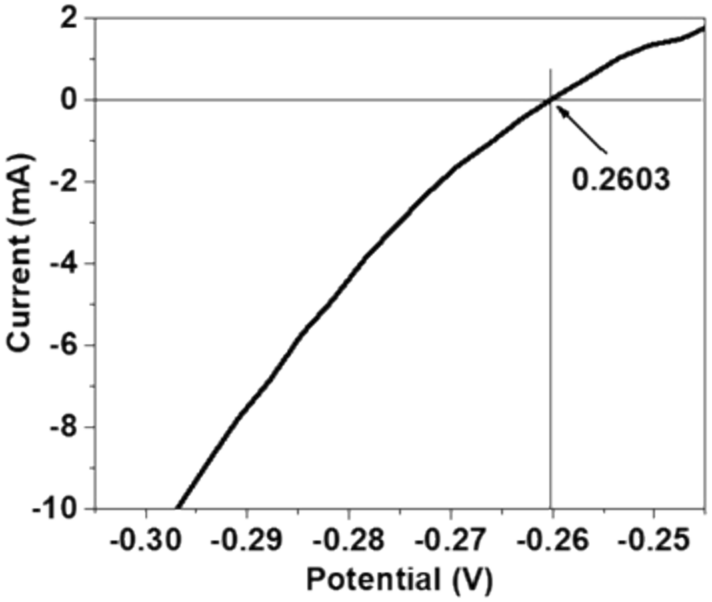

Figure S1. Calibration of SCE with respect to RHE in 0.5 M H_2SO_4 at 1 mV s^{-1}.

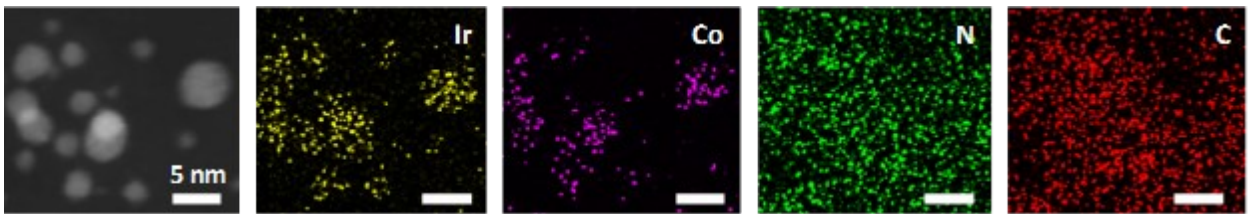

Figure S2. HAADF-STEM image and corresponding element mapping images of IC1-G_N.

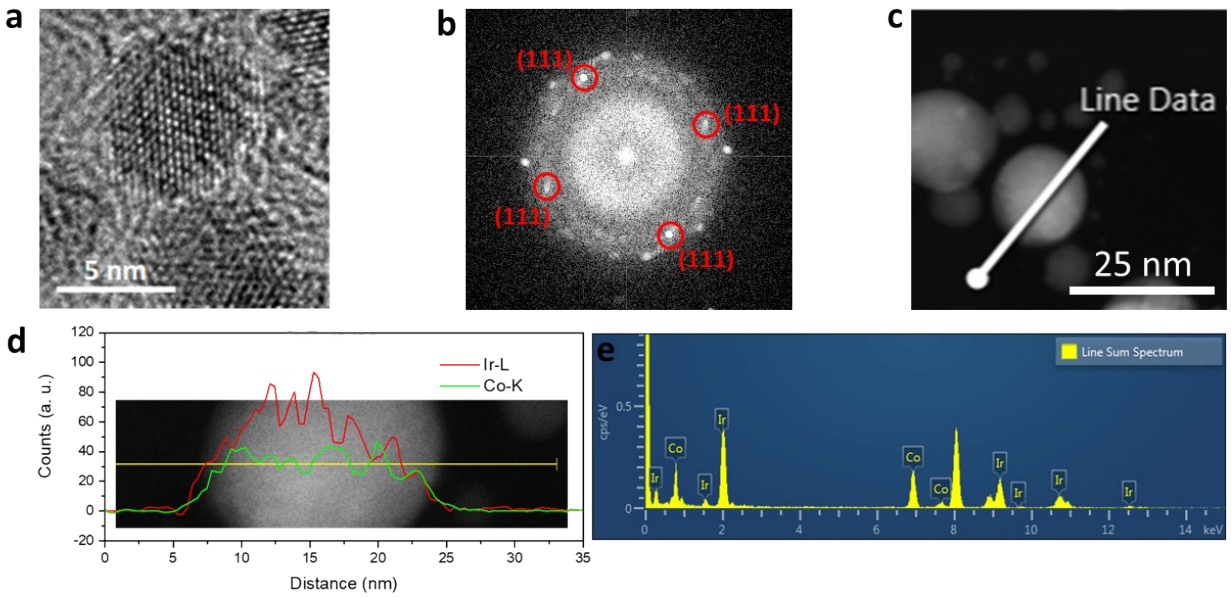

Figure S3. a) HR-TEM image, b) corresponding FFT pattern, c) line EDS mapping, and d-e) concentration profile analyses obtained on the selected line of IC1-G_N. The (111) planes in b) correspond to those of the cubic structure of IrCo alloy, which clearly indicates the formation of IrCo alloy.

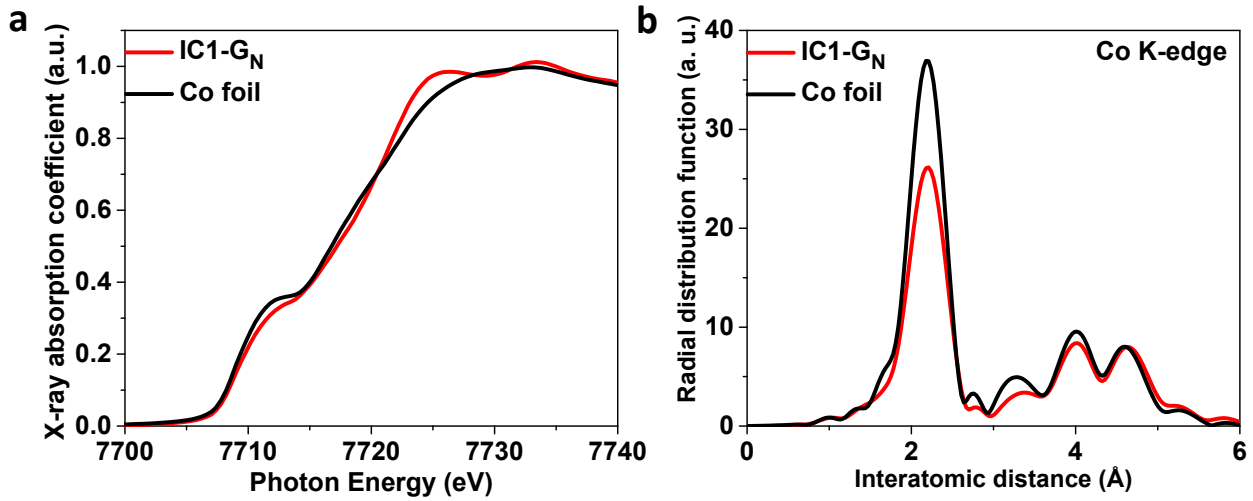

Figure S4. XAFS investigation on the Co moieties at the Co K-edge of IC1-G_N catalyst and Co foil. a) XANES spectra. b) Fourier transform magnitudes.

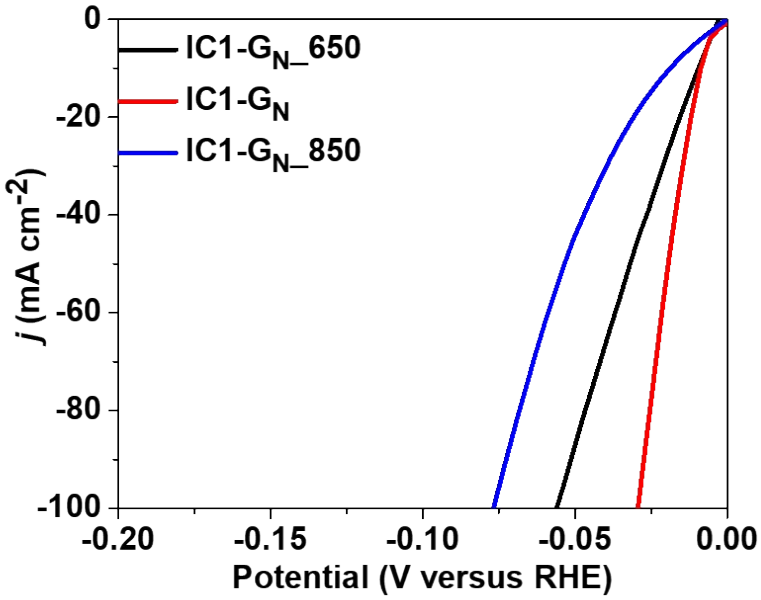

Figure S5. LSV curve of catalysts prepared at different temperatures 650 ^{o}C, 750 ^{o}C, and 850 ^{o}C. In this regard, 750 ^{o}C is the optimized synthesis condition.

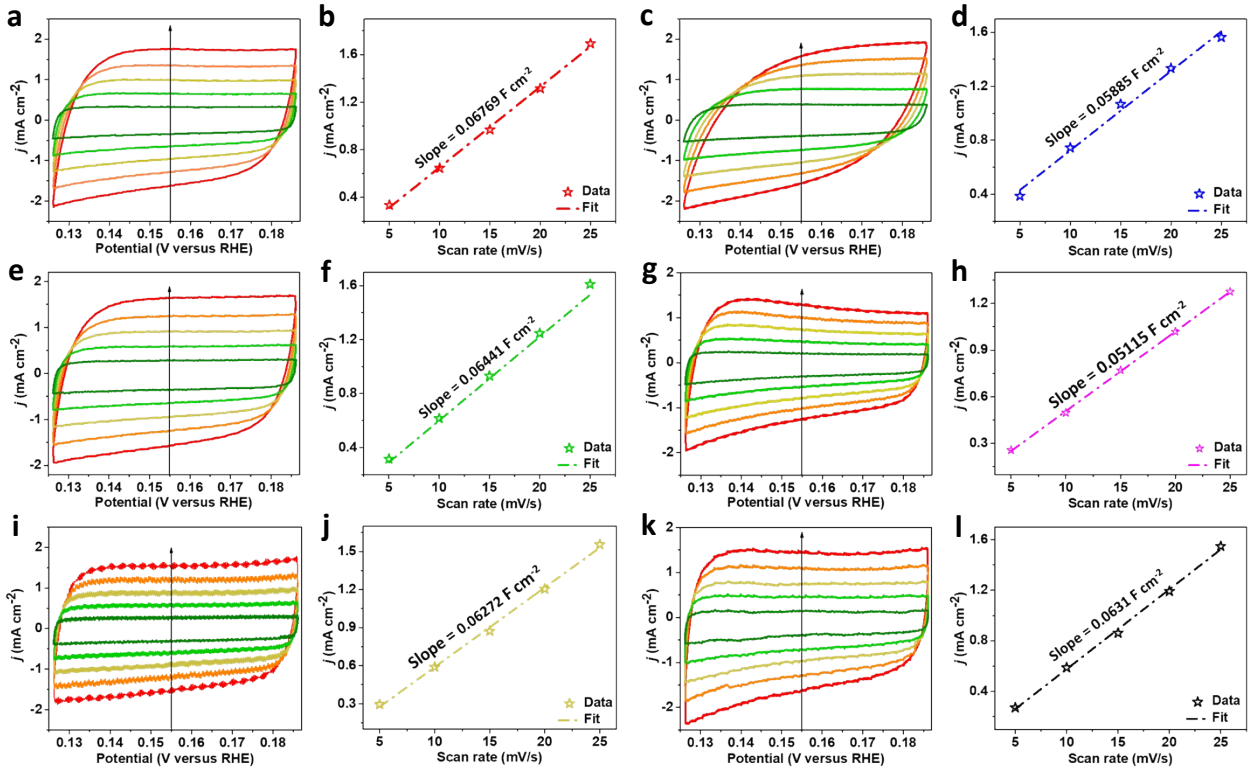

Figure S6. CV profiles recorded in non-Faradaic region with scan rate of 5, 10, 15, 20, 25 mV s^{-1} in H_2-saturated 0.5 M H_2SO_4 electrolyte and corresponding C_{dl} calculation of a,b) IC1-G_N. c,d) IC2-G_N. e,f) IC3-G_N. g,h) IC. i,j) Pt/C. k,l) Ir/C.

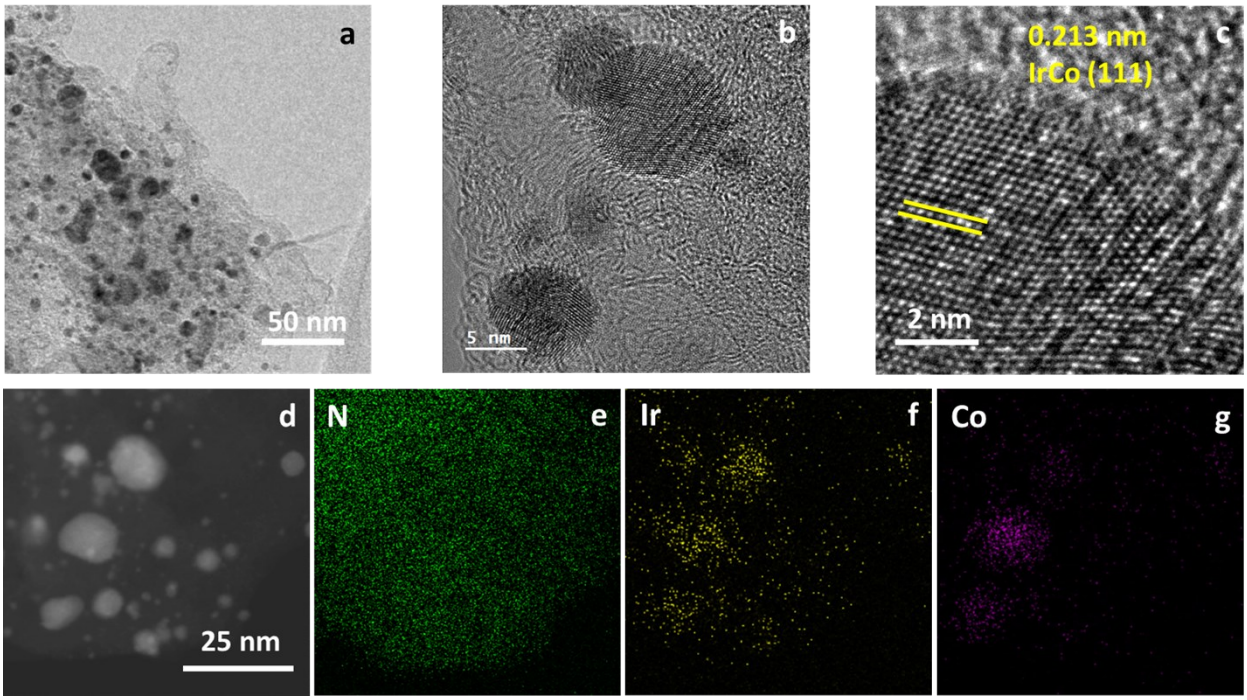

Figure S7. Structural analysis of **IC1-G$_N$** catalyst after stability testing. a) TEM image. b,c) High-resolution TEM images. d) High-angle annular dark-field (HAADF) TEM image and e-h) corresponding elemental mapping of C, N, Ir, Co.

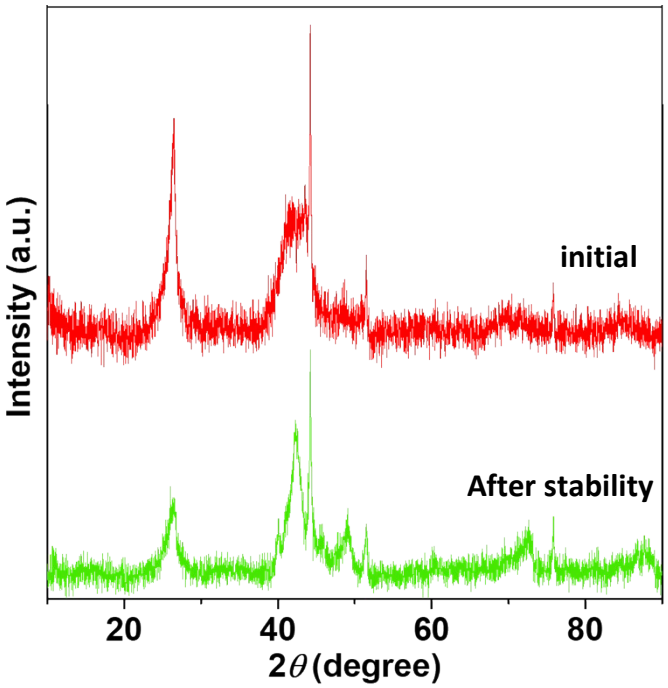

Figure S8. XRD pattern of **IC1-G$_N$** before (red line) and after (green line) stability**.**

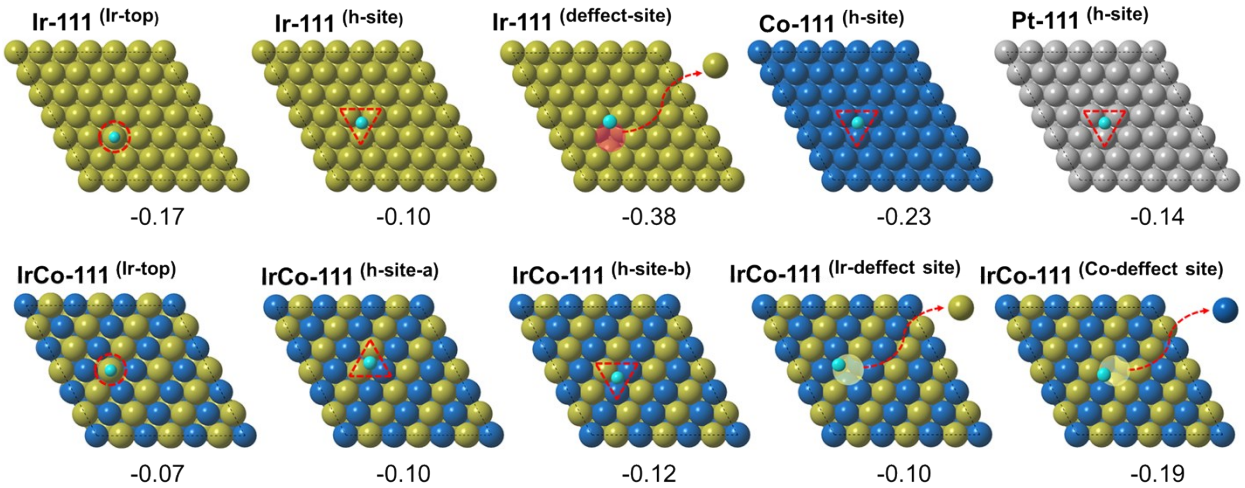

Figure S9. Top view for optimized configurations of most active H-adsorption sites and their corresponding HER-free energy (eV) for different configurations of Ir, Co, Pt, and IrCo. The bulk surfacecs including Ir-111, IrCo-111, Co-111 and Pt-111 surfaces. (Pt: grey, Ir: greenish yellow, Co: light blue, H: cyan).

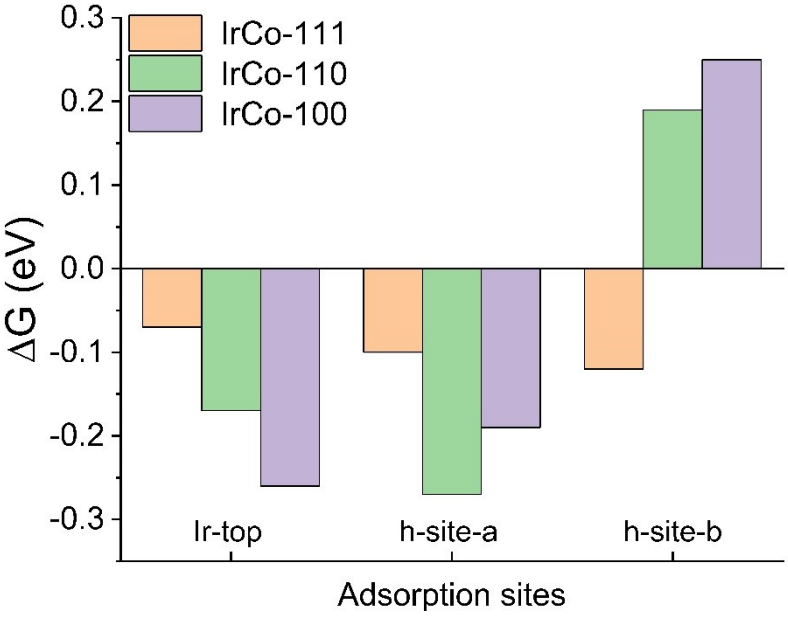

Figure S10. Comparison of HER free energies at different active sites on exposed surfaces of the IC1-G_N electrocatalyst.

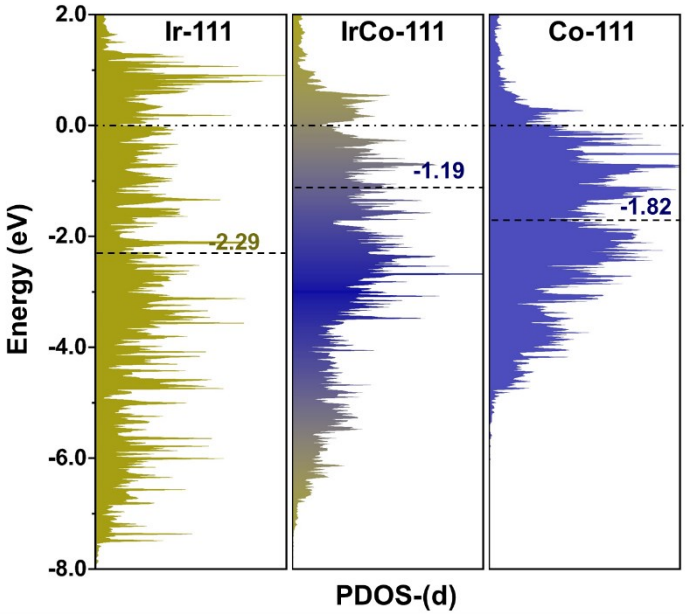

Figure S11. Projected density of states (PDOS) of Ir-111, IrCo-111, and Co-111. The redistribution of d-states in bonding and antibonding causes a slight shift in d-band center towards the Fermi level of IrCo-111 with respect to its parent metals. The charge density map for IrCo-111 is shown in Figure S10 and Figure 4(b). The localized d-electrons near the Fermi level results in an enhanced HER activity.

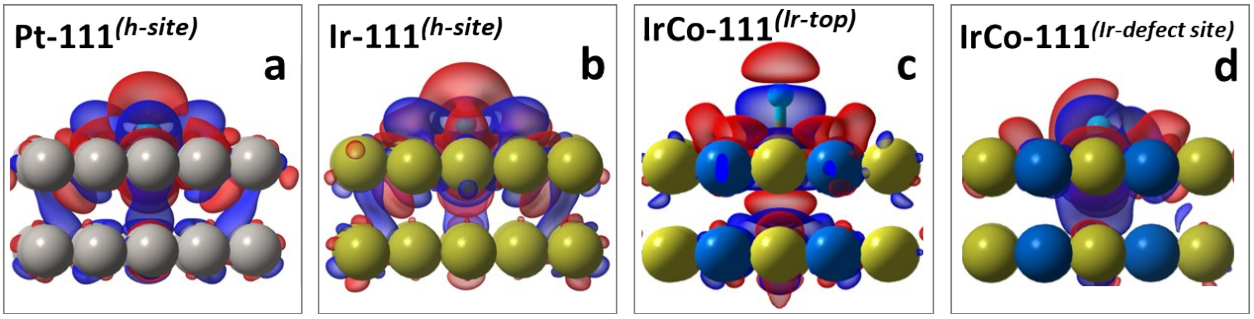

Figure S12. A charge density map (a) Pt-111, (b) Ir-111, (c) 1:1 ratio alloy of IrCo-111, (d) 1:1 ratio alloy of IrCo-111 with defect created by removal of one Ir atom from the surface.

Table S1. The weight percentage of Ir element contained in all catalysts obtained from inductively coupled plasma optical emission spectroscopy (ICP-OES).

Samples	Ir (wt%)	Co (wt%)
IC1-G_N	5.0132	61.354
IC2-G_N	5.3695	46.7463
IC3-G_N	4.8739	88.607
IC	5.0640	64.8959

Table S2. Comparison of the mass activity of IC1-G_N, IC2-G_N, IC3-G_N, IC, commercial Ir/C and Pt/C at 29.3 mV vs RHE.

Catalysts	**Mass activity (A $mg_{Ir\ (or\ Pt)}^{-1}$)**
IC1-G_N	1.662
IC2-G_N	0.773
IC3-G_N	1.615
IC	1.333
Ir/C (20 wt. %)	0.327
Pt/C (20 wt. %)	0.270

Table S3. Comparison of turnover frequency (TOF) values of catalysts.

Samples	**TOF (s^{-1})**
IC1-G_N	1.248
IC2-G_N	0.576
IC3-G_N	1.203
IC	0.989
Ir/C	0.242
Pt/C	0.205

Table S4. ICP-OES analysis of electrolyte after stability testing.

Sample	Ir (mg/L)	Co (mg/L)
IC1-G_N	0.049	0.083

[1]. S. Sultan, J. N. Tiwari, A. N. Singh, S. Zhumagali, M. Ha, C. W. Myung, P. Thangavel, K. S. Kim, *Adv. Energy Mater.,* 2019, **9**, 1900624.

[2]. G. Kresse, J. Furthmüller, *Comput. Mater. Sci.,* 2002, **6**, 15.

[3]. B. Hammer, L. B. Hansen, J. K. Nørskov, *Phys. Rev. B,* 2002, **59**, 7413.

[4]. A. Tkatchenko, M. Scheffler, *Phys. Rev. Lett.,* 2009, **102**, 073005.

[5]. P. E. Blöchl, *Phys. Rev. B,* 2002, **50**, 17953.